

Controlled Micropatterning of a Si(100) Surface by Combined Nitroxide-Mediated and Atom Transfer Radical Polymerizations

F. J. Xu,[†] Y. Song,[‡] Z. P. Cheng,^{†,§} X. L. Zhu,[‡]
C. X. Zhu,[‡] E. T. Kang,^{*,†} and K. G. Neoh[†]

Department of Chemical and Biomolecular Engineering, National University of Singapore, Kent Ridge, Singapore 119260; Department of Electrical and Computer Engineering, National University of Singapore, Kent Ridge, Singapore 117576; and School of Chemistry and Chemical Engineering, Soochow University, Suzhou, P.R. China 215006

Received March 19, 2005

Revised Manuscript Received May 25, 2005

Introduction. Functionalization of oriented single-crystal silicon surfaces with organics is emerging as an important area in the development of new silicon-based devices, such as biomicroelectromechanical systems (BioMEMS), three-dimensional micro- and nanomemory chips, and DNA- and protein-based biochips and biosensors.^{1–6} Stable polymer brushes covalently bonded on a silicon surface can provide excellent mechanical and chemical protection to the substrate, alter the electrochemical characteristics of the interface, and provide new pathways for the functionalization of silicon surfaces.^{2,5–8} Micropatterned polymer brushes are of crucial importance to the development of biochips, microarrays, and microdevices for cell growth, regulation of protein adsorption, and drug delivery.^{1,6,9–12} A variety of techniques, including microlithography^{6,7,9,13} and chemical amplification of patterned monolayers from self-assembly,^{7,10,14,15} have been developed for fabricating patterned polymer brushes.

Nitroxide-mediated radical polymerization (NMRP) and atom transfer radical polymerization (ATRP) have been widely used in the synthesis of well-defined (nearly monodispersed) “living” polymers of controlled molecular weights and macromolecular architecture.^{16–19} ATRP involves a copper halide/nitrogen-based ligand catalyst system,^{16,17} while NMRP is based on a reversible combination of propagating radicals with nitroxide free radicals.^{20,21} It is possible to prepare well-defined polymer brushes on various substrates via surface-initiated NMRP and ATRP.^{22–27} In this communication, different polymer brushes, as well as their diblock copolymer brushes, have been micropatterned on a Si(100) surface via alternating surface-initiated NMRP and ATRP. The ATRP initiator was covalently immobilized via UV-induced hydrosilylation of 4-vinylbenzyl chloride (VBC)²³ with the (HF-etched) hydrogen-terminated silicon (Si–H) microdomains to produce a micropatterned and Si–C bonded VBC monolayer. The NMRP initiator was then introduced in a one-step process¹⁹ onto the unetched (oxide-covered) surface microdomains via reactions with a mixture of the silane coupling agent (3-(trimethoxysilyl)propyl methacrylate (TSPMA)), radical initiator

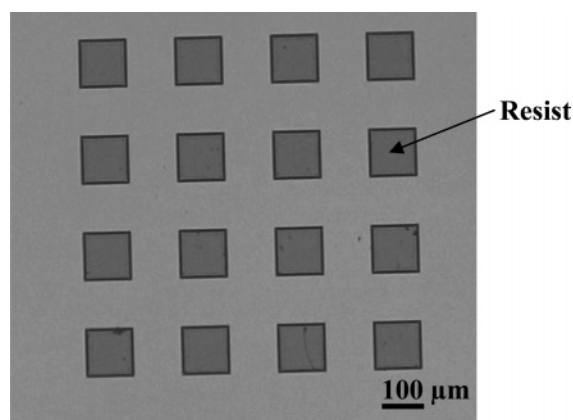


Figure 1. Optical micrograph of the resist-patterned Si(100) surface.

(2,2'-azobis(isobutyronitrile) (AIBN)), and alkoxyamine initiator (2,2,6,6-tetramethylpiperdinyloxy (TEMPO)). This approach to the controlled micropatterning of silicon surfaces via a combination of surface-initiated NMRP and ATRP is shown schematically in Scheme 1.

Experimental Section. The resist-patterned Si(100) chip (Figure 1) of about 1.2 cm × 1.2 cm in size was immersed in 10 vol % HF solution in a Teflon vial for 2 min to remove the oxide film in the resist-free regions and to leave behind a micropatterned Si(100) surface with hydrogen-terminated microdomains (Si–H/SiO₂ surface). Immobilization of the ATRP initiator to the Si–H surface was achieved via 3 min of UV-induced hydrosilylation²³ of VBC with the Si–H surface to produce a Si–C bonded VBC monolayer (Si–VBC/SiO₂ surface). After the UV-induced hydrosilylation reaction, the micropatterned Si–VBC/SiO₂ chip was rinsed with copious amounts of acetone (a good solvent for VBC and the photoresist on the silicon surface) to ensure the complete removal of adsorbed VBC and to expose the SiO₂ regions. Details on the preparation and characterization of the Si–H and Si–VBC surfaces were described earlier.²³ Coupling of the alkoxyamine initiator to the SiO₂ regions¹⁹ of the micropatterned surface was achieved by adding TSPMA (0.41 mmol), AIBN (0.23 mmol), and TEMPO (0.46 mmol) at a molar ratio of 1.8:1:2 into 3 mL of dry DMF in a Pyrex tube containing the Si–VBC/SiO₂ chip. After purging the mixture with argon for 30 min, the surface coupling reaction was conducted at 80 °C for 24 h under an argon atmosphere, followed by introducing 10 μL of water into the reaction mixture. The reaction was conducted for another 24 h to complete the NMRP and ATRP initiator-micropatterned silicon surface (Si–VBC/Si–TEMPO surface). After the reaction, the Si–VBC/Si–TEMPO chip was washed and extracted exhaustively with excess acetone and then with an ethanol/water (1:1, v/v) mixture.

For the preparation of styrene polymer (PS) brushes on the silicon surface, the surface-initiated NMRP of styrene was carried out using a [styrene (48 mmol)]:[AIBN (0.096 mmol)]:[TEMPO (0.192 mmol)] molar feed ratio of 500:1:2 in a Pyrex tube containing the Si–VBC/Si–TEMPO chip. The reaction was conducted at 120 °C for 12 h under an argon atmosphere to produce the Si–VBC/Si-g-PS hybrid. After the reaction, the Si–VBC/Si-

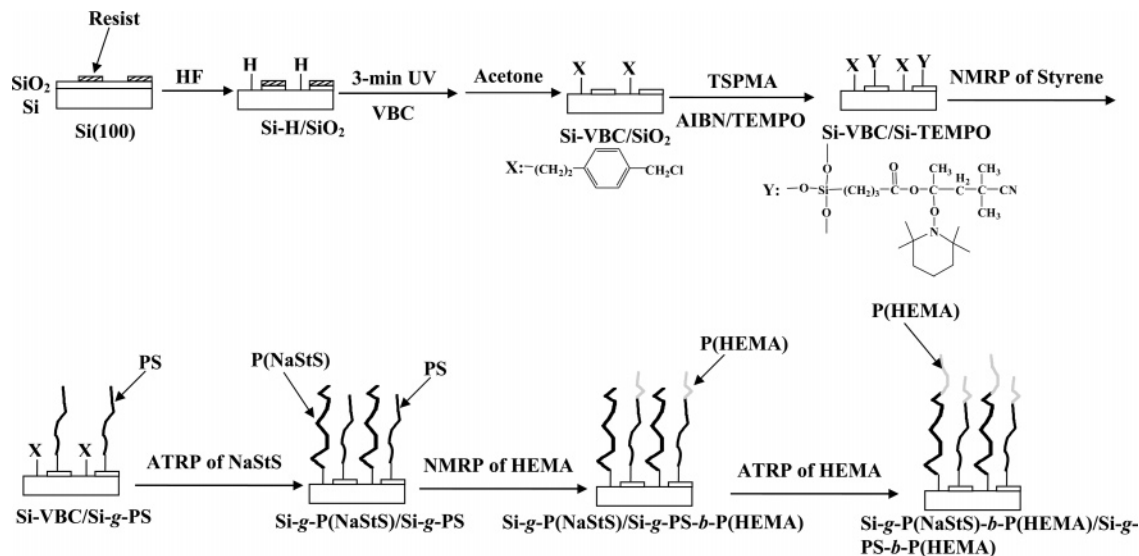
[†] Department of Chemical and Biomolecular Engineering, National University of Singapore.

[‡] Department of Electrical and Computer Engineering, National University of Singapore.

[§] Soochow University.

* To whom all correspondence should be addressed: Tel +65-6874-2189; Fax +65-6779-1936; e-mail cheket@nus.edu.sg.

Scheme 1. Schematic Diagram Illustrating the Process of Controlled Micropatterning of a Silicon Surface by a Combination of Surface-Initiated Nitroxide-Mediated Radical Polymerization (NMRP) and Atom Transfer Radical Polymerization (ATRP)^a



^a VBC = 4-vinylbenzyl chloride, TSPMA = 3-(trimethoxysilyl)propyl methacrylate, AIBN = 2,2'-azobis(isobutyronitrile), TEMPO = 2,2,6,6-tetramethyl-1-piperidinyloxy, PS = polystyrene, NaStS = sodium 4-styrenesulfonate, and HEMA = 2-hydroxyethyl methacrylate.

g-PS hybrid was washed thoroughly with copious amounts of THF and with refluxing dichloromethane to remove the physically adsorbed PS chains on the surface.²⁸ For the preparation of the sodium 4-styrenesulfonate (NaStS) polymer (P(NaStS)) brushes on the VBC-micropatterned section of the Si-VBC/Si-g-PS substrate, the surface-initiated ATRP was carried out using a [NaStS (8.6 mmol)]:[CuCl (0.086 mmol)]:[CuCl₂ (0.0017 mmol)]: [Bpy (0.17 mmol)] molar feed ratio of 100:1:0.2:2 in 5 mL of doubly distilled water in a Pyrex tube containing the Si-VBC/Si-PS chip. The reaction mixture was stirred and degassed with argon for 30 min, prior to being conducted at 50 °C for 12 h to produce the Si-g-P(NaStS)/Si-g-PS hybrid. After the reaction, the Si-g-P(NaStS)/Si-g-PS hybrid was washed thoroughly with doubly distilled water. The micropatterned diblock copolymer brushes on the silicon surface were prepared by using the Si-g-P(NaStS)/Si-g-PS chip as the macro-initiators for the subsequently surface-initiated NMRP and ATRP of the third monomer, 2-hydroxyethyl methacrylate (HEMA). The surface-initiated NMRP of HEMA was carried out using a [HEMA (41 mmol)]:[AIBN (0.082 mmol)]:[TEMPO (0.164 mmol)] molar feed ratio of 500:1:2 in a Pyrex tube containing the Si-g-P(NaStS)/Si-g-PS chip to give rise to the micropatterned Si-g-P(NaStS)/Si-g-PS-b-P(HEMA) hybrid. The surface-initiated ATRP of HEMA was performed using a [HEMA (33 mmol)]:[CuCl (0.33 mmol)]:[CuCl₂ (0.066 mmol)]: [Bpy (0.66 mmol)] molar feed ratio of 100:1:0.2:2 in 4 mL of doubly distilled water at room temperature in a Pyrex tube containing the Si-g-P(NaStS)/Si-g-PS-b-P(HEMA) chip to give rise to the micropatterned Si-g-P(NaStS)-b-P(HEMA)/Si-g-PS-b-P(HEMA) hybrid. The diblock copolymer brushes were washed and extracted thoroughly with ethanol.

Results and Discussion. The composition of modified silicon surfaces was analyzed by X-ray photoelectron spectroscopy (XPS). To avoid cross-contamination of signals from different regions of the micropatterned surface (arising from the limited resolution of the conventional XPS technique), XPS analyses were carried

out on the corresponding large area (nonpatterned) silicon surfaces modified under similar conditions. Details on the preparation and characterization of Si-H and Si-VBC surfaces were described earlier.²³ The resist-patterned Si(100) chip was treated with HF to remove the oxide film in the resist-free region and to leave behind a micropatterned Si-H/SiO₂ surface. For the Si-H surface, no oxidized silicon species in the binding energy (BE) region of 101–103 eV was detected in the Si 2P core-level spectrum, confirming that the silicon surface etched by HF was predominately hydrogen-terminated.^{2,23} The ATRP initiator was immobilized via UV-induced hydrosilylation^{3,23} of VBC with the Si-H region of the Si-H/SiO₂ surface to give rise to a Si-VBC/SiO₂ surface. The presence of UV-induced hydrosilylation of VBC with the Si-H region was ascertained by the XPS wide scan spectrum (Figure 2a) of the Si-VBC control (nonpatterned) surface from UV-induced hydrosilylation under conditions similar to those used for the micropatterned Si-H/SiO₂ surface. A new Cl 2p core-level spectrum at the BE of about 200 eV, characteristic of the covalently bonded chlorine,²³ has appeared. The resist remained intact under the hydrosilylation conditions. A VBC monolayer thickness of about 0.3 nm was immobilized on the Si-H surface. The initiator density and surface initiator efficiency for the Si-VBC surface were estimated to be about 1.4 VBCs/nm² and 35%, respectively.²³

Treatment of the micropatterned Si-VBC/SiO₂ chip with acetone resulted in the removal of the photoresist and exposure of the SiO₂ regions. Uniform silane layers can be coupled on SiO₂ surfaces.^{19,29} Coupling of the alkoxyamine initiator was achieved via a one-step process in the SiO₂ region of the Si-VBC/SiO₂ chip from reactions with a mixture of TSPMA (bearing a terminal double bond), AIBN, and TEMPO (Experimental Section and Scheme 1). During the first 24 h, the reaction of AIBN with the double bond of the TSPMA molecule created a radical intermediate that was trapped in situ by TEMPO to produce the alkoxyamine.¹⁹ Subsequent introduction of a predetermined amount of water into

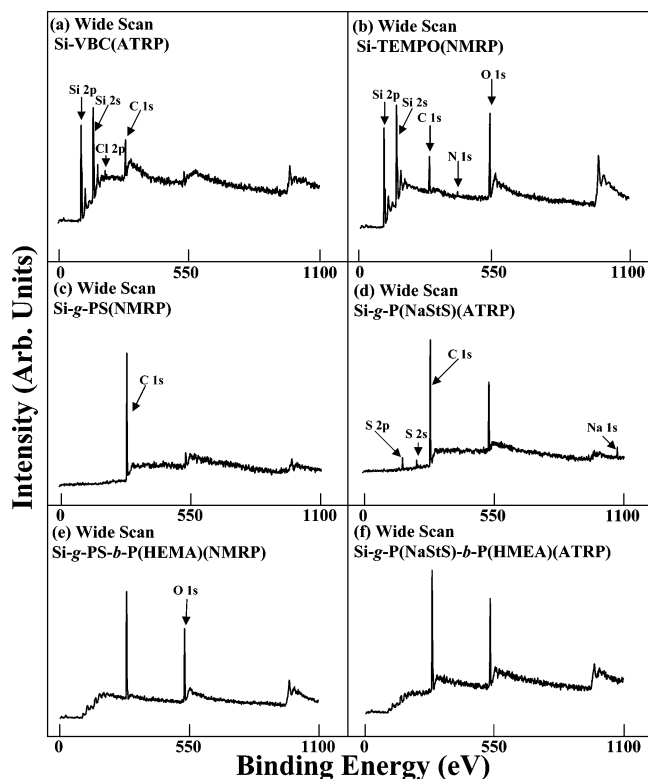


Figure 2. XPS wide scan spectra of the (a) Si-VBC(ATRP), (b) Si-TEMPO(NMRP), (c) Si-g-PS(NMRP), (d) Si-g-P(NaStS)(ATRP), (e) Si-g-PS-*b*-P(HEMA)(NMRP), and (f) Si-g-P(NaStS)-*b*-P(HEMA)(ATRP) surfaces. These silicon surfaces were obtained via surface-initiated NMRP and ATRP from the control (unpatterned) Si(100) substrates. ATRP = atom transfer radical polymerization, VBC = 4-vinylbenzyl chloride, TEMPO = 2,2,6,6-tetramethyl-1-piperidinyloxy, PS = polystyrene, P(NaStS) = poly(sodium 4-styrenesulfonate), and P(HEMA) = poly(2-hydroxyethyl methacrylate).

the reaction mixture is necessary for hydrolysis and for reaction of the silane with the $-OH$ groups in the SiO_2 regions of the patterned Si-VBC/ SiO_2 surface to complete the immobilization of TEMPO (Si-VBC/Si-TEMPO surface). From the parallel experiment on a control Si-VBC surface, the process of TEMPO immobilization did not affect the surface composition of the immobilized VBC layer to a significant extent. The presence of surface-coupled alkoxyamine in the SiO_2 region of the Si-VBC/Si-TEMPO surface is confirmed by the appearance of a new N 1s signal at the BE of 399 eV, characteristic of the neutral amine species,²⁴ in the XPS wide scan spectrum (Figure 2b) of the corresponding Si-TEMPO control surface, prepared from an unpatterned pristine (SiO_2 -covered) silicon chip under conditions similar to those used for the preparation of the Si-VBC/Si-TEMPO surface. On the basis of the surface-coupled alkoxyamine monolayer thickness (h) of about 1.5 nm (determined by ellipsometry), an alkoxyamine density (ρ) of about 1.0 g/cm³, and the alkoxyamine molecular weight (M) of 442 g/mol, the initiator density ($\rho h/M$) for the Si-TEMPO surface was estimated to be about 2 TEMPOs/nm². Figure 3a shows the representative atomic force spectroscopy (AFM) image of the Si-VBC/Si-TEMPO surface. The average vertical distance (VD) (determined by sectional analysis of AFM) between the VBC and TEMPO layers, h_1 , is about 4 nm. Based on the VBC layer thickness of about 0.3 nm and the TEMPO layer thickness of about 1.5 nm, the SiO_2 thickness under the TEMPO layer is about 2.8 nm. This

value is in reasonable agreement with the oxide layer thickness of about 3.0 nm (determined by ellipsometry) for the pristine (oxide-covered) silicon surface.

Styrene, NaStS, and HEMA were selected as the model monomers for the preparation of polymer brushes on the dual-initiator micropatterned silicon surface via surface-initiated NMRP and ATRP. For the surface-initiated NMRP of styrene and HEMA, the addition of a predetermined amount of "free" alkoxyamine initiator to the reaction mixture can help to "control" the surface-initiated polymerization.^{26,28} The molar ratio of [styrene or HEMA]:[AIBN]:[TEMPO] was controlled at 500:1:2. The Cu(II) complex ($CuCl_2$) was added to control the concentration of the deactivating Cu(II) complex^{22,23} during the surface-initiated ATRP of NaStS and HEMA. The molar ratio of [NaStS or HEMA]:[CuCl]:[CuCl₂]:[Bpy] was controlled at 100:1:0.2:2. The presence of grafted styrene polymer (PS), NaStS polymer (P(NaStS)), and HEMA polymer (P(HEMA)) on the silicon surfaces was confirmed by XPS analysis (Figure 2c–f) of the corresponding Si-VBC and Si-TEMPO control (unpatterned) surfaces after the surface-initiated polymerizations. For the surface-initiated NMRP of styrene and block copolymerization of HEMA, the resulting surfaces are referred to as the Si-g-PS(NMRP) and Si-g-PS-*b*-P(HEMA)(NMRP) surfaces, respectively. For the surface-initiated ATRP of NaStS and block copolymerization of HEMA, the resulting surfaces are referred to as the Si-g-P(NaStS)(ATRP) and Si-g-P(NaStS)-*b*-P(HEMA)(ATRP) surfaces, respectively. The disappearance of Si signals in the wide scan spectrum (Figure 2c) of the Si-g-PS(NMRP) surface is consistent with the fact that the thickness of the PS brushes (about 14 nm after 12 h of NMRP) on the silicon surface is larger than the sampling depth of the XPS technique (about 7.5 nm in an organic matrix³⁰). The presence of the S 2p (at the BE of about 167.4 eV),³¹ S 2s (at the BE of about 228 eV),³¹ and Na 1s (at the BE of about 1072 eV)³¹ signals in the wide scan spectrum (Figure 2d) of the Si-g-P(NaStS)(ATRP) surface suggests that P(NaStS) has been successfully grafted from the Si-VBC surface. The thickness of the P(NaStS) brushes (about 21 nm after 12 h of ATRP) is also larger than the sampling depth of the XPS technique. The presence of a strong O 1s (at the BE of about 530 eV)³¹ signal in the wide scan spectrum (Figure 2e) of the Si-g-PS-*b*-P(HEMA)(NMRP) surface suggests that P(HEMA) has been successfully grafted on the Si-g-PS(NMRP) surface. The thickness of the P(HEMA) brushes obtained from 12 h of NMRP was about 9 nm. The disappearance of S signals in the wide scan spectrum (Figure 2f) of the Si-g-P(NaStS)-*b*-P(HEMA)(ATRP) surface is consistent with the fact that the thickness of the P(HEMA) brushes (about 17 nm after 12 h of ATRP) on the Si-g-P(NaStS) surface is larger than the sampling depth of the XPS technique.

Figure 3b,c shows the respective AFM images of the Si-VBC/Si-g-PS surface, obtained at the NMRP time of 12 h from the micropatterned Si-VBC/Si-TEMPO surface, and the Si-g-P(NaStS)/Si-g-PS surface, obtained at the ATRP time of 12 h from the Si-VBC/Si-g-PS surface. The average VD (h_2) between the VBC and PS layers is about 18 nm. Based on the VD (h_1) value of about 4 nm between the VBC and TEMPO layers, the thickness of PS brushes on the Si-VBC/Si-g-PS surface is about 14 nm. A control experiment of "surface-initiated NMRP" of styrene under similar conditions on an unpatterned Si-VBC surface did not produce any

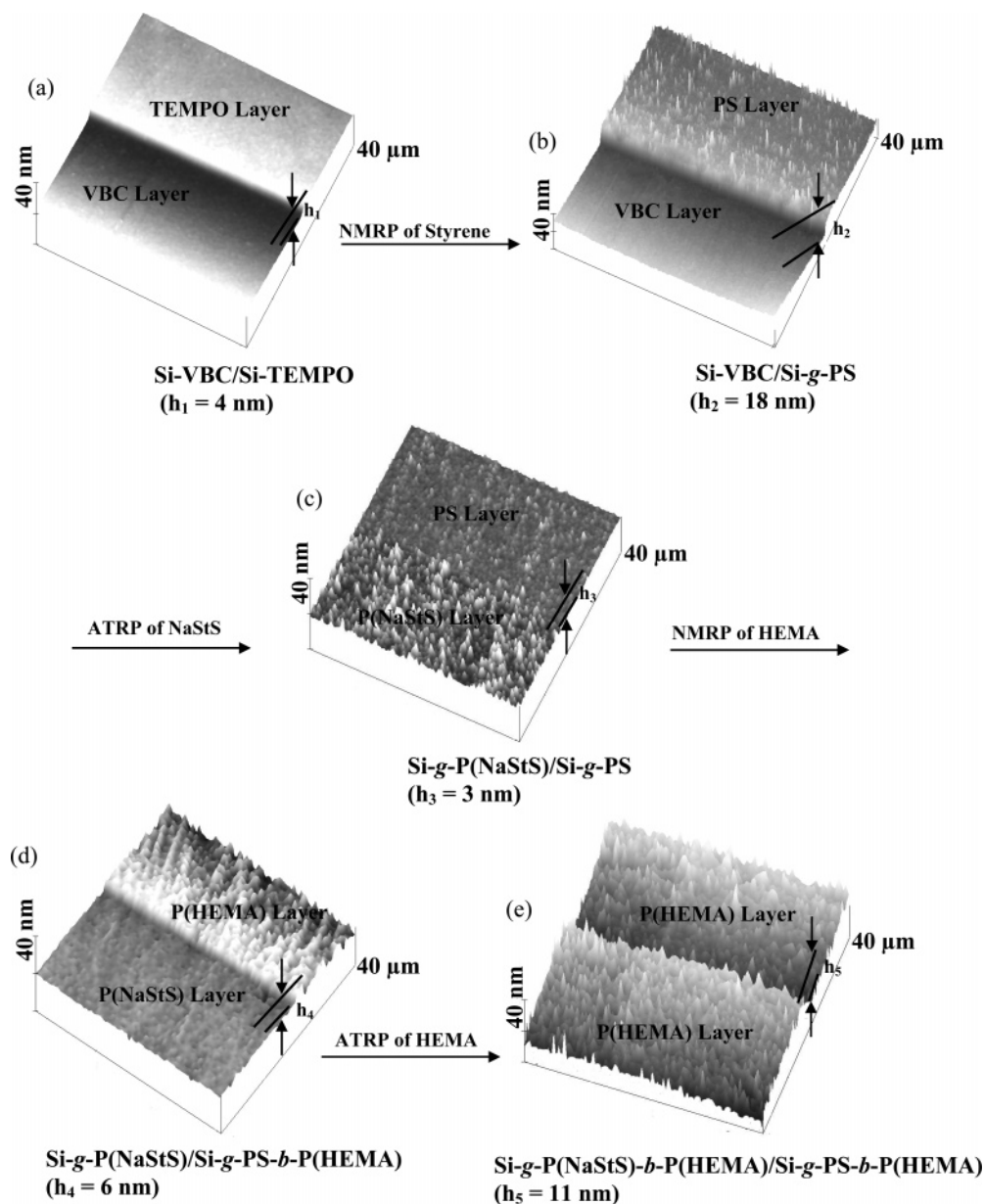


Figure 3. AFM images of the Si-VBC/Si-TEMPO, Si-VBC/Si-g-PS, Si-g-P(NaStS)/Si-g-PS, Si-g-P(NaStS)/Si-g-PS-b-P(HEMA), and Si-g-P(NaStS)-b-P(HEMA)/Si-g-PS-b-P(HEMA) surfaces. VBC = 4-vinylbenzyl chloride, TEMPO = 2,2,6,6-tetramethyl-1-piperidinyloxy, PS = polystyrene, P(NaStS) = poly(sodium 4-styrenesulfonate), and P(HEMA) = poly(2-hydroxyethyl methacrylate). All the AFM images were obtained in the dry state.

significant changes in the organic layer thickness and the relative intensity of the Cl 2p signal. The above results indicate that the C–Cl bond in the ATRP initiator was relatively stable and did not act as a chain transfer agent during NMRP. The average VD (h_3) between the P(NaStS) and PS layers on the Si-g-P(NaStS)/Si-g-PS surface is about 3 nm. Thus, the thickness of P(NaStS) brushes is about 21 nm ($18 + 3 = 21$ nm). A control experiment of “surface-initiated ATRP” of NaStS under similar conditions on an unpatterned Si-TEMPO surface did not produce an increase in organic layer thickness or any significant changes in surface composition.

Polystyrene (PS) brushes exhibit different morphologies, in the dry state, on the Si-VBC/Si-g-PS surface (Figure 3b) and the Si-g-P(NaStS)/Si-g-PS surface (Figure 3c). The former was washed/extracted by THF after the surface-initiated NMRP of styrene from the Si-VBC/Si-TEMPO substrate, while the latter by water after the

surface-initiated ATRP of NaStS from the Si-VBC/Si-g-PS substrate. In addition, the P(NaStS) and PS brushes on the Si-g-P(NaStS)/Si-g-PS surface exhibit obvious phase separation and distinct morphologies.

One of the unique characteristics of the polymers synthesized by NMRP or ATRP is the preservation of active or “living” end groups during the polymerization process. Thus, it is possible to synthesize well-defined block copolymers via a second round of surface-initiated NMRP and ATRP.^{20,23} In this work, a third functional monomer, HEMA, was chosen for the synthesis of diblock copolymer brushes, using the respective PS and P(NaStS) brushes on the micropatterned Si-g-P(NaStS)/Si-g-PS surface as the macroinitiators for the surface-initiated NMRP and ATRP (Scheme 1). Parts d and e of Figure 3 show the respective AFM images of the Si-g-P(NaStS)/Si-g-PS-b-P(HEMA) surface, obtained at 12 h of the surface-initiated NMRP of HEMA from the Si-g-P(NaStS)/Si-g-PS surface, and of the Si-g-P(NaStS)-

b-P(HEMA)/Si-*g*-PS-*b*-P(HEMA) surface, obtained at 12 h of the surface-initiated ATRP of HEMA from the Si-*g*-P(NaStS)/Si-*g*-PS-*b*-P(HEMA) surface. The average VD (h_4) between the P(NaStS) and P(HEMA) layers and VD (h_5) between the P(HEMA) and P(HEMA) layers are about 6 and 11 nm, respectively. The thickness of the P(HEMA) brushes obtained via the surface-initiated NMRP and ATRP are thus about 9 nm ($6 + 3 = 9$ nm, Figure 1d) and 17 nm ($6 + 11 = 17$ nm, Figure 3e), respectively. For the Si-*g*-P(NaStS)/Si-*g*-PS-*b*-P(HEMA) surface (washed/extracted with ethanol), the P(NaStS) and P(HEMA) brushes exhibit distinct morphologies. The two "types" of P(HEMA) brushes on the Si-*g*-P(NaStS)-*b*-P(HEMA)/Si-*g*-PS-*b*-P(HEMA) surface (washed/extracted with ethanol), on the other hand, exhibit a similar morphology.

In summary, micropatterned and well-defined functional polymer brushes of different types have been successfully grafted from a silicon surface by a combination of surface-initiated NMRP and ATRP. The ATRP initiators were covalently immobilized, via robust Si-C bonds, in the H-terminated silicon microdomains, while the NMRP initiators were coupled to the oxide-covered microdomains of the resist-patterned silicon surface. The present two surface-initiated living radical polymerization processes were noninterfering and could be used in combination in the design of well-defined polymer micropatterns with reasonable resolution on an oriented single-crystal silicon surface.

References and Notes

- (1) Lan, S.; Veiseh, M.; Zhang, M. *Biosens. Bioelectron.* **2005**, *20*, 1697–1708.
- (2) Xu, F. J.; Zhong, S. P.; Yung, L. Y. L.; Kang, E. T.; Neoh, K. G. *Biomacromolecules* **2004**, *5*, 2392–2403.
- (3) Buriak, J. M. *Chem. Rev.* **2002**, *102*, 1272–1308.
- (4) Cai, W.; Peck, J. R.; Weide, D. W.; Hamers, R. J. *Biosens. Bioelectron.* **2004**, *19*, 1013–1019.
- (5) Létant, S. E.; Hart, B. R.; Kane, S. R.; Hadi, M. Z.; Reynolds, J. G. *Adv. Mater.* **2004**, *16*, 689–693.
- (6) Iwata, P.; Suk-In, P.; Hoven, V. P.; Takahara, A.; Akiyoshi, K.; Iwasaki, Y. *Biomacromolecules* **2004**, *5*, 2308–2314.
- (7) Zhao, B.; Brittain, W. J. *Prog. Polym. Sci.* **2000**, *25*, 677–710.
- (8) Xu, F. J.; Yuan, Z. L.; Kang, E. T.; Neoh, K. G. *Langmuir* **2004**, *20*, 8200–8208.
- (9) Andruzzi, L.; Senaratne, W.; Hexemer, A.; Sheets, E. D.; Ilic, S. B.; Kramer, J. K.; Baird, B.; Ober, C. K. *Langmuir* **2005**, *21*, 2495–2504.
- (10) Tu, H.; Heitzman, C. E.; Braun, P. V. *Langmuir* **2004**, *20*, 8313–8320.
- (11) Jones, D. M.; Smith, J. R.; Huck, W. T. S.; Alexander, C. *Adv. Mater.* **2002**, *14*, 1130–1139.
- (12) Werne, T. A. V.; Germack, D. S.; Hagberg, E. C.; Sheares, V. V.; Hawker, C. J.; Carter, K. R. *J. Am. Chem. Soc.* **2003**, *125*, 3831–3838.
- (13) Chen, L.; Zhuang, L.; Deshpande, P.; Chou, S. *Langmuir* **2005**, *21*, 818–821.
- (14) Brack, H. P.; Padeste, C.; Slaski, M.; Alkan, S.; Solak, H. *J. Am. Chem. Soc.* **2004**, *126*, 1004–1009.
- (15) Ahn, S. J.; Kaholek, M.; Lee, W. K.; LaMattina, B.; LaBean, T. H.; Zauscher, S. *Adv. Mater.* **2004**, *16*, 2141–2145.
- (16) Coessens, V.; Pintauer, T.; Matayjaszewski, K. *Prog. Polym. Sci.* **2001**, *26*, 337–377.
- (17) Matayjaszewski, K.; Xia, J. H. *Chem. Rev.* **2001**, *101*, 2921–2990.
- (18) He, T.; Li, D.; Sheng, X.; Zhao, B. *Macromolecules* **2004**, *37*, 3128–3135.
- (19) Bartholome, C.; Beyou, E.; Lami, E. B.; Chaumont, P.; Lefebvre, F.; Zydowicz, N. *Macromolecules* **2005**, *38*, 1099–1106.
- (20) Hawker, C. J.; Barclay, G. G.; Dao, J. *J. Am. Chem. Soc.* **1996**, *118*, 11467–11471.
- (21) Hawker, C. J.; Bosman, A. W.; Harth, E. *Chem. Rev.* **2001**, *101*, 3661–3688.
- (22) Pyun, J.; Kowalewski, T.; Matayjaszewski, K. *Macromol. Rapid Commun.* **2003**, *24*, 1043–1059.
- (23) Xu, F. J.; Kang, E. T.; Neoh, K. G. *Macromolecules* **2005**, *38*, 1573–1580.
- (24) Xu, F. J.; Cai, Q. J.; Kang, E. T.; Neoh, K. G. *Macromolecules* **2005**, *38*, 1051–1054.
- (25) Kaholek, M.; Lee, W. K.; Ahn, S. J.; Ma, H.; Caster, K. C.; LaMattina, B.; Zauscher, S. *Chem. Mater.* **2004**, *16*, 3688–3696.
- (26) Zhao, B.; He, T. *Macromolecules* **2003**, *36*, 8599–8602.
- (27) Holmberg, S.; Holmlund, P.; Nicolas, R. Wilen, C. E.; Kallio, T.; Sundholm, G.; Sundholm, F. *Macromolecules* **2004**, *37*, 9909–9915.
- (28) Husseman, M.; Malmstrom, E. E.; McNamara, M.; Mate, M.; Mecerreyes, D.; Benoit, D. G.; Hedrick, J. L.; Mansky, P.; Huang, E.; Russell, T. P.; Hawker, C. J. *Macromolecules* **1999**, *32*, 1424–1431.
- (29) Ingall, M. D. K.; Honeyman, C. H.; Mercure, J. V.; Bianconi, P. A.; Kunz, R. R. *J. Am. Chem. Soc.* **1999**, *121*, 3607–3613.
- (30) Tan, K. L.; Woon, L. L.; Wong, H. K.; Kang, E. T.; Neoh, K. G. *Macromolecules* **1993**, *26*, 2832–2836.
- (31) Moulder, J. F.; Stickle, W. F.; Sobol, P. E.; Bomben, K. D. In *X-ray Photoelectron Spectroscopy*; Chastain, J., Ed.; Perkin-Elmer: Eden Prairie, MN, 1992; pp 40, 47, 62, and 92.

MA050581I